Advances in Engineering Research : Possibilities and Challenges
ISSN Print: 3079-5192
ISSN Online: 3079-5206
https://doi.org/10.63313/AERpc.9010

Simulation and Parameter Influence Study on Metal Pipeline Defect Detection Based on Pulsed Eddy Current

Zhijun Wang*. Mingjiang Shi
School of Mechanical Engineering, Southwest Petroleum University, Chengdu, China
Email: swpu_wzj@163.com

How to cite this paper: Wang, Zhijun, & Shi, Mingjiang. (2025). Simulation and Parameter Influence Study on Metal Pipeline Defect Detection Based on Pulsed Eddy Current. Advances in Engineering Research: Possibilities and Challenges, 1(1), 125-136. ISSN Print: 3079-5192; ISSN Online: 3079-5206.
https://doi.org/10.63313/AERpc.9010
Published: 2025-03-31

Abstract

Metal pipelines, when subjected to prolonged service in complex working environments, are highly susceptible to defects such as corrosion and cracks, which pose significant threats to the safe operation of pipeline systems. Pulsed eddy current testing (PECT), as an emerging non-destructive testing method, offers notable advantages including rapid detection speed, high sensitivity, strong reliability, and non-contact inspection, demonstrating broad application prospects in the field of metal pipeline defect detection. This paper, based on finite element simulation analysis, establishes a PECT simulation model for metal pipeline defects. It investigates the influence of key factors in excitation signal parameters and coil structure parameters on the detection signals, elucidates the relationship between these parameters and detection effectiveness, and provides theoretical foundations and technical references for the optimal design of PECT system parameters and practical engineering applications.

Keywords

Pulsed Eddy Current; Pipeline Defect Detection; Finite Element Simulation; Pa-rameter analysis

1. Introduction

Metal pipelines are widely utilized in industries such as petrochemicals, energy and power, aerospace, and more. Due to their complex operating conditions, they are highly prone to defects such as corrosion and cracks, which can lead to economic losses and even environmental pollution. Currently, common non-destructive testing (NDT) methods for detecting defects in metal pipelines include ultrasonic testing(Ghavamian et al., 2018; Nagy, Simonetti, & Instanes , 2014) (UT), radiographic testing(Li, He, & Li. 2024; Li, Wang, & Zhang, 2019)(RT), magnetic particle testing(Azzura et al.,2019; Wang et al., 2023)(MT), and eddy current testing(Zhang et al., 2019)(ECT). Compared to other methods, eddy current testing offers advantages such as low cost, harmlessness to humans, and the absence of radioactive sources. As a derivative method of eddy current testing, pulsed eddy current (PEC) demonstrates higher detection efficiency and faster inspection speed. By employing square waves as excitation signals, PEC(Cheng, Xu, & Li, 2021; Fang, Shen & Xiong, 2024; Mardaninejad, Safizadeh, 2019)provides richer time-frequency domain information, enabling the detection of more defect details, and thus is widely applied in the inspection of metallic materials.

In pulsed eddy current testing, the excitation signal parameters and the performance of the probe, as the core components of the detection device, directly influence the detection efficiency and accuracy. Therefore, a thorough investigation into the impact of various parameters on the detection results is of significant importance for applying pulsed eddy current to metal pipeline defect detection. Based on this, this paper will utilize the COMSOL Multiphysics finite element analysis software to establish a pulsed eddy current defect detection model for metal pipelines. It will systematically explore the influence of multiple key parameters on detection effectiveness, providing insights for the optimization design of parameters in pulsed eddy current testing.

2. Theoretical basis of pulsed eddy current testing

Maxwell’s equations occupy a central position in the theoretical framework of electromagnetic fields, serving as the fundamental theoretical basis for all work in electromagnetism. Consequently, a thorough understanding of Maxwell’s equations is essential for analyzing the detection mechanisms of pulsed eddy currents.

The differential form of Maxwell’s equations is mathematically expressed as follows:

$$\nabla \times \boldsymbol{H} = \boldsymbol{J} + \frac{\partial \boldsymbol{D}}{\partial t} \tag{1-1}$$

$$\nabla \times \boldsymbol{E} = -\frac{\partial \boldsymbol{B}}{\partial t} \tag{1-2}$$

$$\nabla \cdot \boldsymbol{D} = \rho \tag{1-3}$$

$$\nabla \cdot \boldsymbol{B} = 0 \tag{1-4}$$

In the equations, H represents the magnetic field intensity (A/m), J denotes the current density (A/m2), D is the displacement current vector within the conductor (J/m2), E signifies the electric field intensity (V/m), B stands for the magnetic flux density (T), and ρ represents the free charge density (C/m3). Specifically, Equation (1-1) indicates that at any point in time and space, the circulation of the magnetic field equals the sum of the current density and the time derivative of the displacement current. Equation (1-2) states that the curl of the electric field is the time rate of change of the magnetic flux density. Equation (1-3) demonstrates that the divergence of the electric displacement field equals the charge density, reflecting that electric charges are the source of the electric field. Equation (1-4) confirms that the magnetic field is source-free, affirming the closed nature of magnetic field lines.

To obtain the solutions of Maxwell's equations, it is necessary to further supplement the constitutive relations of the medium. For isotropic and linear media, the constitutive relations are given by the following equations:

$$\boldsymbol{D} = \varepsilon \boldsymbol{E} \tag{1-5}$$

$$\boldsymbol{B} = \mu \boldsymbol{H} \tag{1-6}$$

$$\boldsymbol{J} = \sigma \boldsymbol{E} \tag{1-7}$$

In the equations, ε represents the permittivity of the medium, μ denotes the permeability of the medium, and σ signifies the conductivity of the medium.

By substituting Equations (1-5) through (1-7) into Equations (1-1) through (1-4), the system of equations expressed in terms of field vectors can be further derived:

$$\nabla \times \boldsymbol{H} = \sigma \boldsymbol{E} + \varepsilon \frac{\partial \boldsymbol{E}}{\partial t} \tag{1-8}$$

$$\nabla \times \boldsymbol{E} = -\mu \frac{\partial \boldsymbol{H}}{\partial t} \tag{1-9}$$

$$\nabla \cdot \boldsymbol{E} = \frac{\rho}{\varepsilon} \tag{1-10}$$

$$\nabla \cdot \boldsymbol{H} = 0 \tag{1-11}$$

Based on the aforementioned equations, it is theoretically feasible to calculate the electromagnetic field distribution of any test specimen under various inspection conditions. In pulsed eddy current testing, by specifying particular excitation signal parameters and incorporating the intrinsic electromagnetic properties of the test specimen, the overall magnetic field distribution within the inspected space can be determined using the above equations. Consequently, the magnetic field distribution can be further utilized to analyze the defect characteristics of the specimen.

3. Finite element simulation model

The COMSOL Multiphysics model for pulsed eddy current defect detection in metal pipelines is established as illustrated in Fig.1 (the air domain and infinite element domain have been hidden). Considering the symmetry of the pipeline, only half of the pipe body was constructed during modeling to reduce computational load. The complete model consists of a metal pipeline, an excitation coil, a sensing coil, and an air domain. Specifically, a ferromagnetic pipeline was used to simulate the test pipeline, while a combination of the excitation coil and sensing coil was employed to model the detection probe.

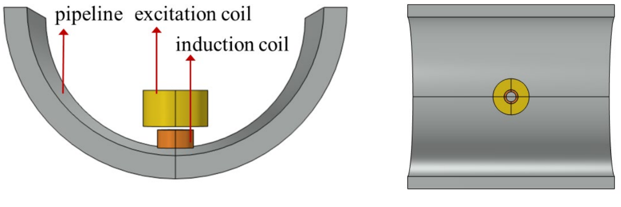

(a) Model front view (b) Model top view

Fig.1 Three-dimensional simulation model without defects

The key parameters of the solid models in the three-dimensional simulation are summarized in Table 1.

Table 1 The key parameters of each solid model in the simulation model

model parameter	parameter declaration	model parameter	parameter declaration
Pipeline outer diameter	178 mm	Pipeline inner diameter	154 mm
Pipeline length	200 mm	Pipeline relative permeability	150
Pipeline electrical conductivity	4×10^6 S/m	Outer diameter of excitation coil	38 mm
Inner diameter of excitation coil	14 mm	Thickness of excitation coil	20 mm
Excitation coil turns	250 turns	Wire diameter of excitation coil	0.2 mm
Air relative permeability	1	Air domain diameter	400 mm
Air electrical conductivity	1 S/m	Outer diameter of induction coil	20 mm
Inner diameter of induction coil	10 mm	Thickness of induction coil	10 mm
Induction coil turns	500 turns	Wire diameter of induction coil	0.1 mm
Coil vertical spacing	1 mm	Probe lift-off distance	1 mm

In COMSOL Multiphysics, a unipolar square wave voltage is defined as the excitation signal, with its amplitude, duty cycle, and frequency set to 10 V, 0.4, and 100 Hz, respectively. The waveform of the generated excitation signal and the response waveform measured by the sensing coil under defect-free conditions are illustrated in Fig2. For ease of analysis, the peak value of the positive induced voltage is adopted for investigation in the subsequent sections.

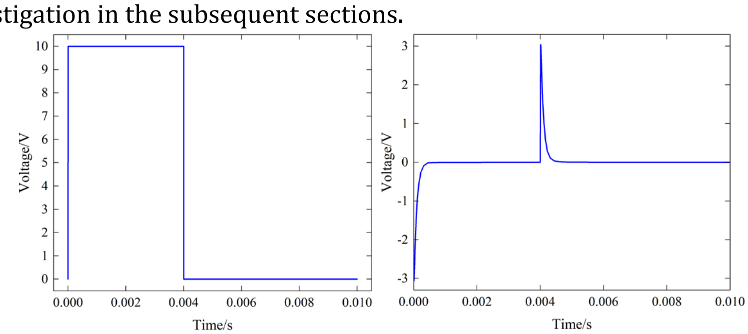

(a) Excitation signal (b) Response signal

Fig.2 Excitation signal and response signal

4. Influence parameter analysis

To investigate the influence of various parameters on the detection effectiveness in pulsed eddy current testing, multiple sets of simulation experiments were conducted under both defect-free and defective conditions based on the initial parameters described earlier, utilizing the control variable method. For the defective experiments, a rectangular groove with a width of 14 mm and a depth of 4 mm was consistently set to represent the surface defect of the pipeline. During detection, the probe was positioned vertically and directly aligned with the center of the defect, as illustrated in Fig.3.

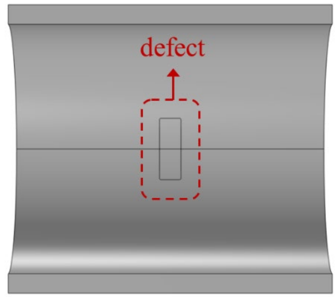

Fig.3 Simulation model of pipeline with defects

4.1. Influence of excitation signal parameters

1) The influence of excitation signal amplitude on the detection results

The amplitude of the excitation signal was varied from 5 V to 30 V, and simulation experiments were conducted under both defect-free and defective conditions. The measured induced voltage signals and excitation currents are shown in Fig.4. Here, “def” represents the detection results under defective conditions, while “nodef” denotes the detection results under defect-free conditions (the same applies hereafter).

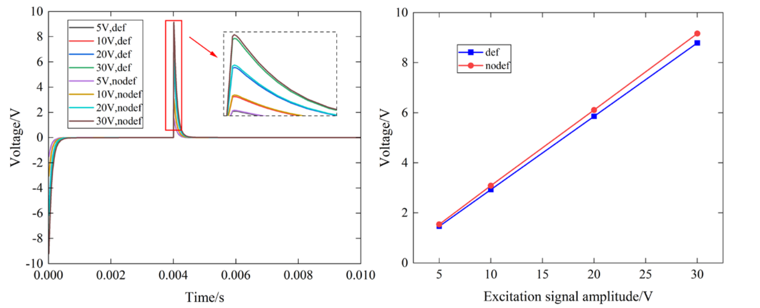

(a) Induced voltage (b) Change of induced voltage peak value

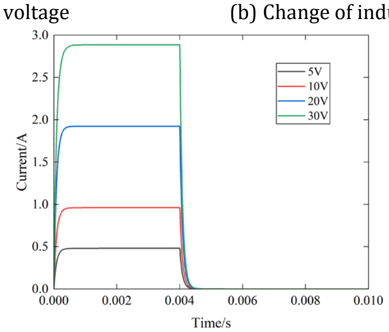

(c) Excitation current

Fig.4 Simulation results under different excitation signal amplitudes

As illustrated in Fig.4(a) and Fig.4(b), the peak value of the induced voltage increases linearly with the amplitude of the excitation voltage under both defect-free and defective conditions. Therefore, enhancing the amplitude of the excitation signal can improve detection sensitivity. However, as analyzed in Fig.4(c), increasing the amplitude of the excitation signal simultaneously leads to a rise in the current within the excitation coil, thereby generating greater heat. Consequently, to ensure detection effectiveness and prevent coil burnout, it is essential to judiciously select the amplitude of the excitation voltage.

2) The influence of excitation signal frequency on detection results

While keeping other parameters unchanged, the frequency of the excitation signal was varied from 10 Hz to 100 Hz, and simulation experiments were conducted under both defect-free and defective conditions. The measured induced voltage signals and excitation currents are shown in Fig.5.

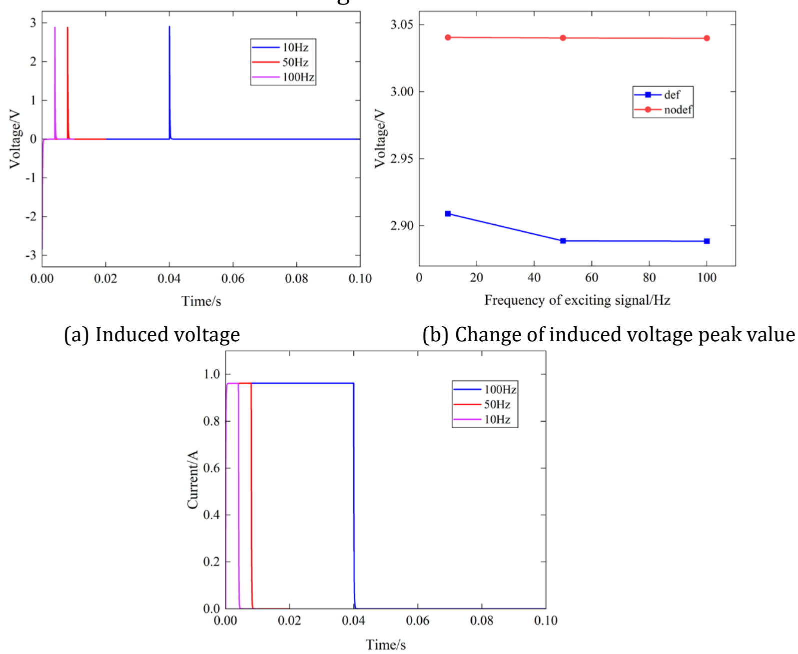

(a) Induced voltage (b) Change of induced voltage peak value

(c) Excitation current

Fig.5 Simulation results under different excitation signal frequencies

As shown in Fig.5(a) and Fig.5(b), under defect-free conditions, the induced voltage is almost unaffected by the frequency of the excitation signal. However, under defective conditions, the peak value of the induced voltage exhibits a slight decreasing trend as the excitation signal frequency increases, indicating that higher-frequency excitation signals exhibit greater sensitivity to surface defects. From Fig.5(c), it is evident that while the amplitude of the excitation current is not significantly influenced by the excitation signal frequency, the duration of the excitation current is noticeably altered.

3) The influence of excitation signal duty cycle on detection results

While keeping other parameters unchanged, the duty cycle of the excitation signal was varied from 20% to 60%, and simulation experiments were conducted under both defect-free and defective conditions. The measured induced voltage signals and excitation currents are shown in Fig.6.

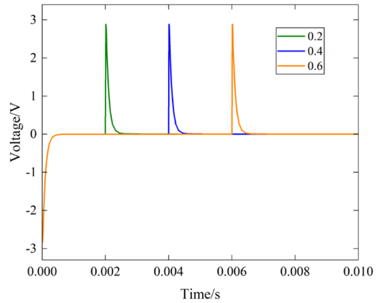

(a) Induced voltage

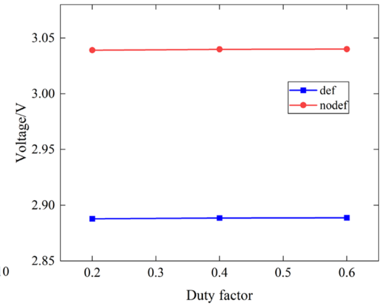

(b) Change of induced voltage peak value

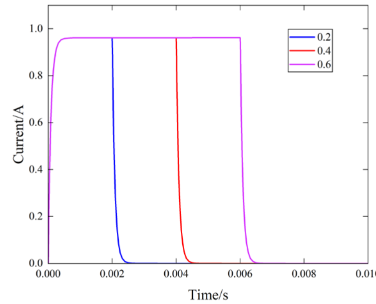

(c) Excitation current

Fig.6 Simulation results under different excitation signal duty cycles

As illustrated in Fig.6(a) and Fig.6(b), under both defective and defect-free conditions, variations in the duty cycle of the excitation signal have minimal impact on the peak value of the induced voltage. However, under defective conditions, the peak value of the induced voltage is generally lower than that under defect-free conditions. From Fig.6(c), it is evident that the duty cycle of the excitation signal directly influences the duration of the excitation current.

4.2. The influence of excitation coil parameters

1) The influence of excitation coil inner diameter on detection results

While keeping other parameters unchanged, the inner diameter of the excitation coil was varied from 10 mm to 24 mm, and simulation experiments were conducted under both defect-free and defective conditions. The measured induced voltage signals and excitation currents are shown in Fig.7.

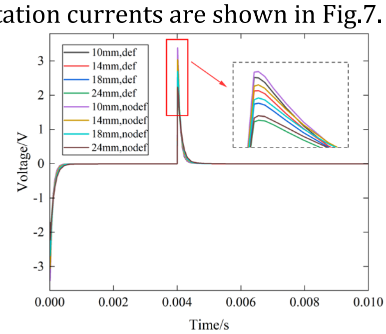

(a) Induced voltage

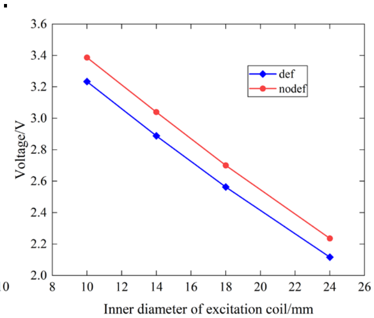

(b) Change of induced voltage peak value

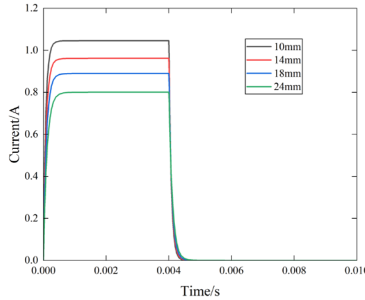

(c) Excitation current

Fig.7 Simulation results under different excitation coil inner diameters

As shown in Fig.7(a) and Fig.7(b), the inner diameter of the excitation coil also significantly affects the peak value of the induced voltage. Under both defective and defect-free conditions, the peak value of the induced voltage decreases linearly as the inner diameter of the excitation coil increases. This indicates that excitation coils with smaller inner diameters exhibit higher sensitivity, while those with larger inner diameters may be less effective for distinguishing subtle defects. Analysis of Fig.7(c) reveals that, within a certain range, the excitation current increases as the inner diameter of the excitation coil decreases. Therefore, excitation coils with smaller inner diameters offer greater detection sensitivity but also result in higher currents, leading to increased heat generation.

2) The influence of excitation coil thickness on detection results

While keeping other parameters unchanged, the thickness of the excitation coil was varied from 16 mm to 22 mm, and simulation experiments were conducted under both defect-free and defective conditions. The measured induced voltage signals and excitation currents are shown in Fig.8.

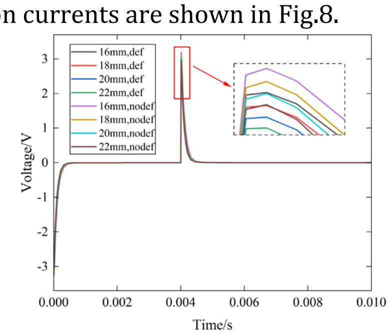

(a) Induced voltage

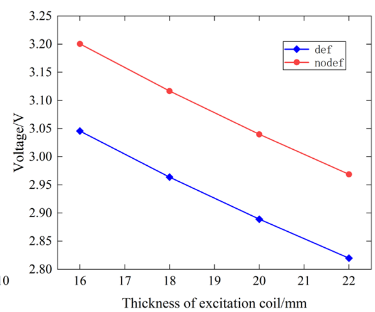

(b) Change of induced voltage peak value

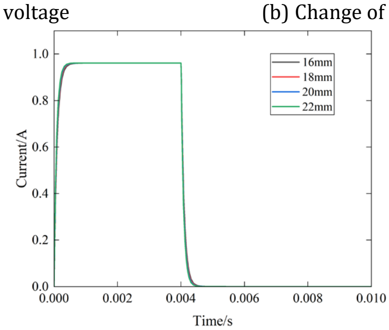

(c) Excitation current

Fig.8 Simulation results under different excitation coil thicknesses

As shown in Fig.8(a) and Fig.8(b), under both defective and defect-free conditions, the peak value of the induced voltage gradually decreases as the thickness of the excitation coil increases. Analysis of Fig.8(c) reveals that excitation coils of different thicknesses exhibit similar behavior in terms of excitation current, with nearly identical current peaks. This indicates that the thickness of the excitation coil has a relatively minor influence on the excitation current.

3) The influence of excitation coil turns on detection results

While keeping other parameters unchanged, the number of turns of the excitation coil was varied from 250 turns to 1500 turns, and simulation experiments were conducted under both defect-free and defective conditions. The measured induced voltage signals and excitation currents are shown in Fig.9.

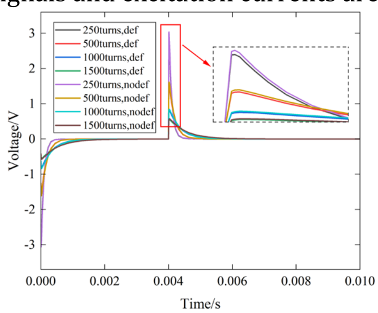

(a) Induced voltage

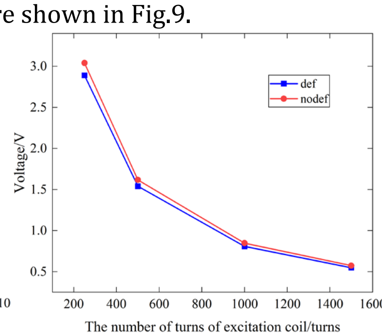

(b) Change of induced voltage peak value

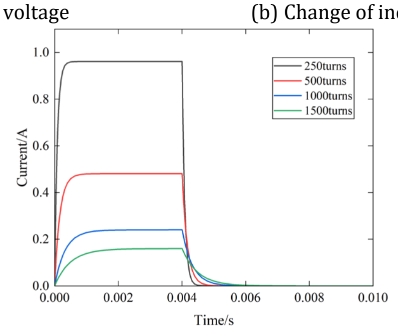

(c) Excitation current

Fig.9 Simulation results under different excitation coil turns

As shown in Fig.9(a) and Fig.9(b), the number of turns of the excitation coil has a significant impact on the peak value of the induced voltage. The peak value of the induced voltage decreases markedly as the number of turns of the excitation coil increases, indicating that, within a certain range, excitation coils with fewer turns exhibit higher sensitivity to defect detection. Fig.9(c) demonstrates that, within a certain range, excitation coils with fewer turns generate larger excitation currents. Therefore, while excitation coils with fewer turns may be more sensitive to defect detection, they also produce more heat. Conversely, excitation coils with a higher number of turns generate smaller excitation currents, but the excitation current decays more slowly after the excitation signal is turned off, exhibiting a more pronounced inductive effect. Consequently, excitation coils with a higher number of turns may be less suitable for rapid-response defect detection.

4.3. The influence of sensing coil parameters

Since the simulation model employs a coaxial top-bottom coil probe configuration, and to avoid affecting the distance between the excitation coil and the pipeline surface, this study focuses solely on analyzing the inner diameter and number of turns of the sensing coil, while other sensing coil parameters are not discussed. Additionally, as the sensing coil is primarily used to convert changes in the magnetic field into voltage, the current in the sensing coil is not a primary focus of this research and is therefore not analyzed.

1) The influence of sensing coil inner diameter on detection results

While keeping other parameters unchanged, the inner diameter of the sensing coil was varied from 6 mm to 12 mm, and simulation experiments were conducted under both defect-free and defective conditions. The measured induced voltage signals are shown in Fig.10.

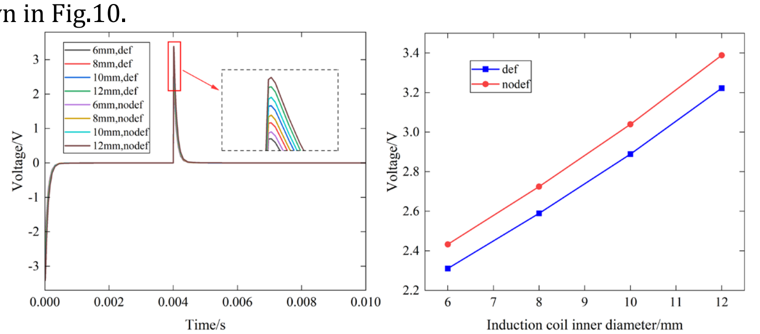

(a) Induced voltage (b) Change of induced voltage peak value

Fig.10 Simulation results under different sensing coil inner diameters

As shown in Fig.10(a) and Fig.10(b), the inner diameter of the sensing coil has a significant impact on the peak value of the induced voltage. The peak value of the induced voltage increases linearly with the inner diameter of the sensing coil, indicating that appropriately increasing the inner diameter of the sensing coil can significantly enhance the peak value of the positive induced voltage, thereby improving signal strength and detection effectiveness.

2) The influence of sensing coil turns on detection results

While keeping other parameters unchanged, the number of turns of the sensing coil was varied from 500 turns to 2000 turns, and simulation experiments were conducted under both defect-free and defective conditions. The measured induced voltage signals are shown in Fig.11.

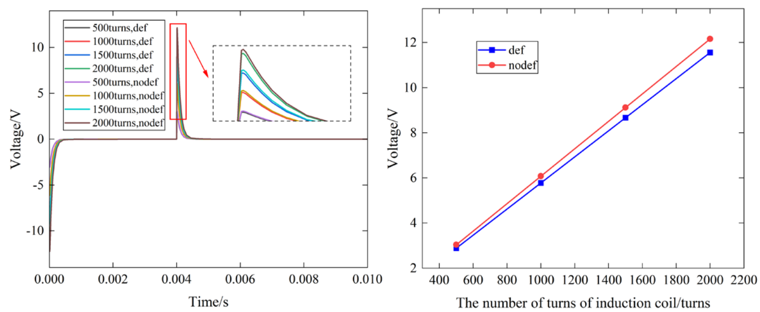

(a) Induced voltage (b) Change of induced voltage peak value

Fig.11 Simulation results under different sensing coil turns

As shown in Fig.11(a) and Fig.11(b), the peak value of the induced voltage exhibits an almost linear growth relationship with the number of turns of the sensing coil. This indicates that appropriately increasing the number of turns of the sensing coil can effectively enhance the strength of the induced signal, making the detection results clearer and more robust. Therefore, appropriately increasing the number of turns of the sensing coil is beneficial for more accurately identifying and distinguishing defects in the material.

5. Conclusion

This study establishes a finite element simulation model for pulsed eddy current defect detection in metal pipelines based on COMSOL Multiphysics finite element analysis software, and conducts an in-depth investigation into the influence of multiple key parameters. The results indicate that: (1) From the perspective of the excitation signal, increasing the amplitude of the excitation voltage can effectively enhance the peak value of the induced voltage, but the current-carrying capacity of the enameled wire and the resulting thermal effects must be considered; (2) High-frequency signals are more sensitive to surface defects, while the duty cycle primarily affects the duration of the excitation current. (3) From the perspective of coil parameters, appropriately reducing the inner diameter, thickness, and number of turns of the excitation coil can improve sensitivity but also increase coil heating; (4) Conversely, appropriately increasing the inner diameter and number of turns of the sensing coil can enhance the strength of the induced signal and improve defect identification capability.

References

[1] Azzura I, Farhana M S N, Lokman M N, Mahzan S, Ahmad S, Taib H, et al.(2019). Identification Corrosion Hydrogen Attack on Carbon Steel Using Magnetic Particle Inspection (MPI). International Conference On Mechanical Engineering Research And Application, 494, 012059. doi:10.1088/1757-899X/494/1/012059

[2] Cheng Jingui, Xu Lei, Li Chao.(2021). A review of two types of non-destructive testing technique for pressure pipelines. Insight, 63(6): 326-333. https://doi.org/10.1784/insi.2021.63.6.326

[3] Fang Jie, Shen Jialong, Xiong Lei.(2024). Modelling and experimental study on pipeline

defect characterisations using a pulsed eddy current measurement. Nondestructive Testing And Evaluation, 1-23. https://doi.org/10.1080/10589759.2024.2413693

[4] Ghavamian A, Mustapha F, Baharudin B T H T, &Yidris N.(2018). Detection, localisation and assessment of defects in pipes using guided wave techniques: A Review. Sensors (Basel, Switzerland), 18(12): 4470. https://doi.org/10.3390/s18124470

[5] Li Hui, Wang Yongan, Zhang Xiaodong.(2019). Research Progress on an Intelligent X-ray Backscattering Nondestructive Testing Robot for the Internal Inspection of Petroleum Pipelines. 2019 IEEE Nuclear Science Symposium and Medical Imaging Conference (NSS/MIC). doi: 10.1109/NSS/MIC42101.2019.9059791

[6] Li Hui, He Liang, Li Hua, Li Deyuan.(2024). Simulation of defect detection for the buried petroleum pipe by the X-ray backscatter imaging. APPLIED Radiation And Isotopes, 207, 111278. https://doi.org/10.1016/j.apradiso.2024.111278

[7] Mardaninejad R, Safizadeh M S.(2019). Gas Pipeline Corrosion Mapping Through Coating Using Pulsed Eddy Current Technique. Russian Journal Of Nondestructive Testing, 55(11): 856-867. https://doi.org/10.1134/S1061830919110068

[8] Nagy P B, Simonetti F, Instanes G.(2014). Corrosion and erosion monitoring in plates and pipes using constant group velocity Lamb wave inspection. Ultrasonics, 54: 1832-1841. https://doi.org/10.1016/j.ultras.2014.01.017

[9] Wang Gang, Li Yuting, Xiao Qi, Li Wenhui.(2023). Finite element study of remote field eddy current methods for inner diameter and outer diameter pipeline defect classification.Insight, 65(3): 139-145. https://doi.org/10.1784/insi.2023.65.3.139

[10] Zhang Wei, Li Yanjun, Shi Yibing, Xiao Siwei, Li Zhipeng.(2019). Finite element simulation analysis of influencing factors in near field eddy current testing. Proceedings Of 2019 14TH IEEE International Conference On Electronic Measurement \& Instruments (ICEMI), 992-1000. doi: 10.1109/ICEMI46757.2019.9101695